N89-20960

COMPARISON OF AIRFOIL RESULTS FROM AN ADAPTIVE WALL TEST SECTION AND A POROUS WALL TEST SECTION

Raymond E. Mineck
NASA Langley Research Center
Hampton, Virginia

SUMMARY

Two wind tunnel investigations have been conducted to assess two different wall interference alleviation/correction techniques: adaptive test section walls and classical analytical corrections. The same airfoil model has been tested in the adaptive wall test section of the NASA Langley 0.3-Meter Transonic Cryogenic Tunnel (TCT) and in the National Aeronautical Establishment (NAE) High Reynolds Number Two-Dimensional Facility. The model has a 9-inch chord and a CAST 10-2/DOA 2 airfoil section. The 0.3-m TCT adaptive wall test section has four solid walls with flexible top and bottom walls. The test section is 13 inches by 13 inches at the entrance. The ratio of the TCT test section height to the model chord is 1.4. The NAE test section has porous top and bottom walls and solid side walls. It is 15 inches wide and 60 inches tall. The ratio of the NAE test section height to model chord is 6.7.

This report compares the aerodynamic results corrected for top and bottom wall interference at Mach numbers from 0.3 to 0.8 at a Reynolds number of 10×10^6. Movement of the adaptive walls was used to alleviate the top and bottom wall interference in the test results from the NASA tunnel. Classical analytical techniques were used to correct the test results from NAE tunnel for top and bottom wall interference. Selected chordwise pressure distributions and the integrated force and moment coefficients are presented for common test conditions. A comparison of the slope of the normal force curves, the drag rise characteristics, and the upper surface shock locations is also included. A portion of the results has been corrected for sidewall interference. These experimental results are then compared with analytically predicted free air results.

The shock locations were in very good agreement. The slopes of the normal force curves and the drag levels were in reasonable agreement except at the highest Mach numbers. The adaptive wall used for the NASA tests alleviated the top and bottom wall interference to produce results in reasonable agreement with the analytically corrected results from the NAE tests.

INTRODUCTION

The interference of test section walls on the flow field around a model introduces an error in the measurements from wind tunnel tests. In two-dimensional airfoil tests, different types of interference arise from the top and bottom walls and from the sidewalls. Corrections are applied to wind tunnel test results to account for the wall interference. These corrections are relatively simple for tests in closed test sections at low subsonic speeds. However, the corrections become more complex and difficult to apply for tests in ventilated test sections at high subsonic speeds. The difficulties involve mathematically modeling and experimentally measuring the flow field at the wall. The digital computer has aided the development of sophisticated wall correction techniques for ventilated test sections at high subsonic speeds. These techniques often depend on extensive measurements taken on or near the test section boundaries. Several examples of these techniques used for two-dimensional testing are presented in reference 1. The digital computer has also aided the development of adaptive wall test sections which have the potential of removing the wall interference at its source. Free air results can be approached using a post-test wall correction technique, a real-time adaptive wall test section technique, or some combination of the two techniques.

The National Aeronautical Establishment (NAE) of Canada and the National Aeronautics and Space Administration (NASA) have a cooperative agreement to develop and validate methods to correct or alleviate wall interference in transonic two-dimensional wind tunnel testing at high Reynolds number. Both organizations desired to verify wall interference correction methods for data obtained at high subsonic speeds and high Reynolds numbers. The same model was tested in both wind tunnels. The corrected results could then be compared to assess each correction technique. The NAE used an analytical wall correction technique for airfoil data from its High Reynolds Number Two-Dimensional Facility. NASA used an adaptive wall test section technique for airfoil data from its 0.3-m Transonic Cryogenic Tunnel (TCT).

Under the cooperative agreement, the NAE designed and fabricated a CAST 10-2/DOA 2 airfoil model with a 9-inch chord. This airfoil profile was chosen because it has aerodynamic characteristics sensitive to changes in Mach number and Reynolds number. The model was tested in both tunnels at Mach numbers from 0.3 to 0.8 at chord Reynolds numbers of 10, 15, and 20 x 10^6. The angle of attack varied from about -2^o to stall. The airfoil model was first tested in the NAE High Reynolds Number Two-Dimensional Facility. This tunnel, described in references 2 and 3, has a 15-inch by 60-inch test section with perforated top and bottom walls. The ratio of the NAE test section height to the model chord was 6.7 for this test. The relatively large ratio was expected to lead to moderate levels of wall interference. The results from the NAE tests, presented in reference 4, were corrected for top and bottom wall interference using the method of reference 5.

The same model was then tested in the NASA Langley 0.3-m TCT with the two-dimensional, adaptive wall test section. Details of the tunnel may be found in reference 6. A description of the test section may be found in reference 7. The 13-inch by 13-inch test section has four solid walls with flexible top and bottom walls. The ratio of TCT test section height to model chord was 1.4. This small ratio would be expected to lead to large levels of wall interference unless the flexible walls were properly positioned. The results from the 0.3-m TCT tests, presented in reference 7, were corrected for top and bottom wall interference by the movement of the adaptive walls. The wall adaptation technique used for this test is described in reference 8.

This report compares the aerodynamic results corrected for top and bottom wall interference at a Reynolds number of 10 x 10^6. Selected chordwise pressure distributions and the integrated force and moment coefficients are presented for common test conditions. A comparison of the slope of the normal force curves, the drag rise characteristics, and the upper surface shock locations is also included. A selected portion of both sets of results has been corrected for sidewall interference. These experimental results are compared with analytically predicted free air results.

SYMBOLS

c	model chord, inches
c_d	section drag coefficient, measured on tunnel centerline

c_m	section pitching moment coefficient, resolved about the 0.25c
c_n	section normal force coefficient
$c_{n,c}$	section normal force coefficient corrected for sidewall interference
c_{n_α}	slope of section normal force coefficient curve, deg^{-1}
$c_{d,c}$	section drag coefficient corrected for sidewall interference
c_{n,c_α}	slope of section normal force coefficient curve corrected for sidewall interference, deg^{-1}
C_p	local pressure coefficient
M_∞	free stream Mach number
$\bar{M}_\infty$	average free stream Mach number for a set of data
$M_{\infty,c}$	free stream Mach number corrected for sidewall interference
NAE	NAE Two-Dimensional High Reynolds Number Facility
NASA	NASA Langley 0.3-Meter Transonic Cryogenic Tunnel
R_c	free stream Reynolds number based on model chord
Tun	Tunnel used for experiments
u	non-dimensional disturbance velocity in x direction due to test section walls
u_c	non-dimensional computed disturbance velocity in x direction
u_m	non-dimensional measured disturbance velocity in x direction
v	non-dimensional disturbance velocity in y direction due to test section walls
v_c	non-dimensional computed disturbance velocity in y direction
x	chordwise position, measured aft from leading edge, inches
x_s	chordwise position of shock on upper surface, measured aft from leading edge
y	adaptive wall displacement or distance normal to free stream direction
z	model vertical ordinate, positive up
α	geometric angle of attack, degrees
β	Prandtl-Glauert compressibility factor, $\sqrt{1 - M_\infty^2}$
γ	ratio of specific heats

Γ	strength of vortex
Δy	change in adaptive wall displacement
$\Delta y'$	change in slope of adaptive wall
$\Delta\alpha$	Correction to angle of attack due to top and bottom wall interference
ΔM_∞	Correction to Mach number due to top and bottom wall interference
μ	strength of doublet
η	transformed co-ordinate in y direction
ξ	transformed co-ordinate in x direction or dummy variable of integration
φ	disturbance potential
φ_m	disturbance potential from model boundary
φ_w	disturbance potential from wall boundary

WIND TUNNELS

NASA Langley 0.3-Meter Transonic Cryogenic Tunnel

The NASA tests used the Langley 0.3-m TCT with the adaptive wall test section. The 0.3-m TCT is a fan-driven, cryogenic pressure tunnel which uses gaseous nitrogen as the test gas. It is capable of continuous operation at stagnation temperatures from about 80K to 327K and at stagnation pressures from 1.2 atmospheres to 6.0 atmospheres. The fan speed is variable so that the empty test section Mach number can be varied from about 0.20 to 0.95. This combination of test conditions provides a test envelope of chord Reynolds numbers up to about 100 x 10^6 based on a model chord of 12 inches. Additional details of the tunnel may be found in reference 6.

A sketch of the adaptive wall test section with the test section plenum wall removed is presented in figure 1. The test section is 13 inches by 13 inches in cross section at the entrance. All four walls are solid. The sidewalls are rigid and parallel. The top and bottom walls are flexible and movable. The test section portion of the flexible wall is 55.8 inches long. The flexible walls are anchored at the upstream end. The shape of each wall is determined by 21 independent jacks. Pressure orifices are located at each jack position on each flexible wall centerline. The model is supported between two turntables centered 30.7 inches downstream of the test section entrance. The sidewall boundary layer removal system, shown in figure 1, was not used in this test. Further details of this test section may be found in reference 7.

A total head probe rake was installed 17.5 inches downstream of the center of the turntable. This location was 1.2 chords downstream of the model trailing edge. The rake had 6 total pressure probes positioned across the left half of the test section. The drag data presented in this report was computed from the data from the probe on the test section centerline.

No traditional model upright and inverted tests of flow angularity and no empty test section tests with a flow angularity probe have been conducted in the adaptive wall test section. Therefore, no corrections for flow angularity have been made to the angle of attack, α.

NAE Two-Dimensional High Reynolds Number Facility

The NAE tests used the 5-ft x 5-ft Blowdown Wind Tunnel with the Two-Dimensional High Reynolds Number Facility test section. Details of the tunnel and the test section may be found in references 2 and 3. The tunnel with the two-dimensional test section typically operates at stagnation pressures up to about 10 atmospheres and at stagnation temperatures near room temperature. The test section Mach number can be varied from about 0.10 to 0.95. These test conditions provide a test envelope of chord Reynolds number up to 50×10^6 based on a model chord of 12 inches. The air storage system provides run times from 5 to 60 seconds depending on the test conditions.

A sketch of the two-dimensional test section is presented in figure 2. The test section is 15 inches wide and 60 inches high at the entrance and is 141 inches long. The sidewalls are solid and parallel. The porous top and bottom walls are also parallel. The porous walls are covered with a 30 mesh, 40.8-percent open screen to reduce the edgetone noise. The resulting overall porosity of the walls is 8.4 percent. A 1-inch diameter static pressure tube is mounted on the centerline of the top wall and the bottom wall. There are 40 static pressure taps on the tube. The pressure orifice locations extend from 80.9 inches upstream to 47.1 inches downstream of the model center of rotation. The center of rotation is located on the centerline, 94 inches downstream of the start of the test section. The model is mounted on a porous turntable within an 18-inch by 24-inch porous panel covered with a woven wire sheet. The porous panel is connected to a suction box to control the boundary layer in the vicinity of the model. The suction is intended to control the adverse growth of the boundary layer from the pressure signature imposed on the sidewall by the model. It is not intended to remove completely the boundary layer. A suction velocity (nondimensionalized by the free stream velocity) of 0.0085 was chosen for these tests. Previous tests have shown that this value is sufficient to prevent premature separation of the sidewall boundary layer in the region of adverse pressure gradients.

A total head probe rake is mounted 21 inches downstream of the center of the turntable. For the 9-inch chord airfoil used in this test, this location corresponds to 1.78 chords downstream of the trailing edge. The rake had four total head probes. The drag data presented in this report was computed from the data from the probe on the test section centerline.

The flow angularity in the NAE test section is very small. Measurements taken before the latest improvements to the tunnel indicate a downwash of about 0.05°. The current flow angularity is expected to be even smaller. No correction to the angle of attack for test section flow angularity has been applied to the results.

MODEL

The model used in these tests has a 9-inch chord and a CAST 10-2/DOA 2 airfoil section which is 12.2 percent thick. The design and measured airfoil ordinates are presented in table 1. A photograph of the model is given in figure 3. The model has a 15-inch span to fit the NAE test section. Since the 0.3-m TCT test section is 13 inches wide, the outer 1 inch on each end of the model extended into the model mounting blocks as shown. With this arrangement, the model centerline and the test section centerline coincided for both tests.

The model chord line was defined as the line passing from the center of the leading to the center of the trailing edge. This line is rotated 0.88° nose up relative to the reference line used to define the airfoil shape. For these tests, α was referenced to the model chord line. Care is needed when comparing these CAST 10-2/DOA 2 airfoil results to other CAST 10-2/DOA 2 results because some tests have referenced α to the line $z = 0$ used to define the airfoil shape.

The model is equipped with 45 pressure orifices in a chordwise row on the upper surface and 23 orifices in a chordwise row on the lower surface. Two spanwise rows of 6 orifices were installed. One row was on the upper surface. The other row was on the lower surface. The orifices in the chordwise row are staggered about the model centerline to minimize interference on the neighboring orifices. The orifices from the leading edge back to the 22-percent chord are 0.010 inches in diameter. All other orifices are .014 inches in diameter. Smaller orifices are used over the forward portion of the airfoil to reduce any orifice size effects where the pressure gradients could be large.

TEST PROGRAM

The test program was designed to assess test section wall interference alleviation and correction techniques in an adaptive wall tunnel and a passive wall tunnel. The test program was not intended to determine airfoil performance. Previous tests of a CAST 10-2/DOA 2 airfoil section in the ONERA T2 adaptive wall tunnel show the shock locations differ significantly for fixed and free transition at a chord Reynolds number of 13×10^{6} (reference 9). At the Reynolds numbers planned for these tests, tunnel turbulence levels could influence the boundary layer characteristics and the shock location. Since the primary purpose of these tests was to evaluate two wall interference alleviation and correction techniques using two different tunnels, the effect of tunnel turbulence on transition and shock location had to be removed from the experiments. Therefore, both tests were conducted with transition strips on both surfaces of the model. The grit size was determined using the method of reference 10 for a Reynolds number of 10×10^{6}. Carborundum grit no. 320 with average grit size of .0011-inches was used for both tests. The 0.1-inch wide transition strip was located at the 5-percent chord.

The range of Mach numbers was from 0.3 to 0.8 at chord Reynolds numbers of 10, 15, and 20×10^{6}. The range of α was from about -2° through stall. The wall positioning hardware in the NASA 0.3-m TCT could not reach the required displacement for successful wall adaptation for some of the higher α's. The NASA tests do not include results up to the stall angle for many of the test conditions. The α's chosen for the NASA tests were selected to obtain data at the same normal force coefficients achieved in the NAE tests.

INTERFERENCE ALLEVIATION AND CORRECTION TECHNIQUES

Wall Adaptation Technique for the NASA Tests

This section presents a summary of the wall adaptation technique used to alleviate the interference of the top and bottom walls of the NASA results. The alleviation is achieved by proper movement of the top and bottom flexible walls. Further details of the method may be found in reference 8. As shown in figure 4, the flow field is split into two regions: a real flow field inside a control surface near the test section walls and an imaginary flow field extending from the control surface to infinity in both directions. The control surface, or the effective wall position, is the physical wall position plus the displacement thickness of the boundary layer.

Finding the proper flexible wall position is an iterative process. The wall position and the wall static pressure are measured at each jack station. The tangential perturbation velocity at the control surface is determined from the measured pressure coefficient. The wall position and the tangential velocity are converted to the incompressible equivalent, $y(x)$ and $u_m(x)$, using the Prandlt-Glauert compressibility factor. The wall shape for the imaginary flow field is set to the measured incompressible wall shape and the potential flow over this wall shape is computed. The potential flow solution is used to compute the horizontal perturbation velocity, $u_c(x)$. The wall slope is assumed to be small. Therefore, the computed perturbation $u_c(x)$ is assumed to be parallel to the control surface. The difference between the measured, u_m, and the computed ,u_c, velocity perturbations can be treated as a vortex sheet.

$$\Gamma(x) = u_m(x) - u_c(x)$$

For small wall slopes, the downwash, $v_c(x)$, induced by the vortex sheet can be determined by integration as follows

$$v_c(x) = \frac{1}{2\pi}\int_{-\infty}^{\infty}\frac{\Gamma(\xi)}{x-\xi}\,d\xi$$

The wall shape will be a streamline if the downwash is zero (no normal flow). This can be done by redirecting the free stream through the appropriate angle to cancel the computed downwash. For small wall slopes, the angle is the non-dimensional vertical perturbation velocity.

$$\Delta y'(x) = -v_c(x)$$

The change in wall displacement is found by integration from the wall anchor point.

$$\Delta y(x) = \int_0^x \Delta y'(\xi)\,d\xi$$

The change in wall displacement is converted to the compressible equivalent and the wall positioned to the new shape. This process is repeated until a set of convergence criteria are satisfied. The convergence criteria are presented in table 2. Once the convergence criteria are satisfied, the data are recorded.

The wall adaptation technique determines the wall position from wall pressures measured on the centerline of the top and bottom walls. No pressures are measured off the centerline. The flow field in the test section can be three dimensional and successful adaptation can still take place.

Analytical Correction Technique for the NAE Tests

This section presents a summary of the analytical technique used to correct the NAE results for interference from the top and bottom walls only. Details of the technique may be found in reference 5. The NAE correction technique assumes the flow field at the test section boundaries can be represented by potential flow theory with linearized compressibility effects. This type of flow can reasonably be expected for the long length and large ratio of test section height to model chord for the NAE test section and the typical airfoil test Mach numbers. An axis system is defined with the origin located at the quarter chord of the model. A rectangular control surface, shown in figure 5, is defined with the corners at the most upstream and downstream pressure orifices on the top wall and bottom wall static pipes. If this control surface is far from the model, the compressible potential equation can be used to represent the flow field near the control surface.

$$\beta^2 \varphi_{xx}(x,y) + \varphi_{yy}(x,y) = 0$$

The disturbance potential can be decomposed into two parts, one part due to the wall and the other part due to the model.

$$\varphi(x,y) = \varphi_w(x,y) + \varphi_m(x,y)$$

The part due to the model can be represented by a series of singularities representing the model lift, blockage, and wake. The model lift is represented by a vortex, the blockage by a doublet, and the wake by a source. The wake is assumed to be small because attached flow on the model is assumed. If there was massive separation and a large wake, two dimensional flow would not be expected and the data would be questionable. Therefore, the source term is ignored. The resulting series for the perturbation potential of the model is

$$\varphi_m(x,y) = -\frac{\Gamma}{2\Pi} \tan^{-1} \frac{\beta y}{x} + \frac{\mu}{\Pi\beta} \frac{x}{x^2 + (\beta y)^2}$$

The strength of the vortex is determined from the model lift coefficient. The strength of the doublet is determined from the model cross-sectional area. By stretching the x co-ordinate by $1/\beta$, the governing equation is transformed into the Laplace equation in a new (ξ,η) coordinate system.

$$\varphi_{\xi\xi}(\xi,\eta) + \varphi_{\eta\eta}(\xi,\eta) = 0$$

$$\text{where: } \xi = \frac{x}{\beta}$$

$$\eta = y$$

The derivatives of solutions of Laplace are also solutions to Laplace's equation. Thus, the perturbation velocity in the x direction also satisfies Laplace's equation.

$$u_{\xi\xi}(\xi,\eta) + u_{\eta\eta}(\xi,\eta) = 0$$

$$\text{where: } u(\xi,\eta) = \varphi_{w_\xi}(\xi,\eta) = \beta\varphi_{w_x}(\xi,\eta)$$

The boundary condition is obtained from

$$u(\xi,\eta) = -\beta\left(\tfrac{1}{2}C_p(x,y) - \varphi_{m_x}(x,y)\right)$$

The perturbation potential from the model is known from the integrated lift coefficient and the model cross-sectional area. The pressure coefficient is measured on the top and bottom sides of the control surface. No measurements of the pressure coefficient on the upstream and downstream faces of the control surface are available. If these faces are far enough from the model, the missing measured pressures can be approximated by linearly interpolating between the measured values at the corners. Thus, the Laplace equation for the perturbation velocity and the boundary conditions on all sides of control surface form a Dirichlet problem that can be solved by the Fast Fourier Transform method. The solution for the perturbation velocity take the form of a Fourier sine series with coefficients determined from the boundary conditions. The correction to the Mach number is

$$\Delta M_{\infty} = \left(1 + \frac{\gamma - 1}{2} M_{\infty}^{2} \right) \varphi_{w_x} = \left(1 + \frac{\gamma - 1}{2} M_{\infty}^{2} \right) M_{\infty} \quad u$$

The perturbation velocity, u, is evaluated at the quarter chord point on the model. The correction to α is

$$\Delta\alpha = v(\xi,\eta) = \varphi_{w_y}$$

The vertical interference velocity can be obtained by integrating as follows

$$v(\xi,\eta) = \int u_{\eta}(\xi,\eta)\ d\eta = -\int u_{\xi}(\xi,\eta)\ d\eta$$

The integral is evaluated from some reference point to the model quarter chord. The resulting constant of integration is a function of the location of the chosen reference point and the flow direction at that point with the tunnel empty.

The applied corrections to α and the Mach number have been plotted in figure 6. The correction to α increases with normal force coefficient and is a weak function of Mach number. The correction to the Mach number is dependent on both the Mach number and the normal force coefficient. As expected from the large test section height to model chord ratio, the magnitude of these corrections is moderate. The level of uncertainty in the results after these corrections have been applied should be only a fraction of the correction.

DISCUSSION OF RESULTS

Results Corrected for Top and Bottom Wall Interference

The measured aerodynamic data consisted of chordwise static pressure distributions on the airfoil model and loss of momentum in the model wake. Many of the chordwise pressure distributions from the two tests have been compared. Two samples are presented in figure 7. These samples represent the worst and best agreement of the results. The agreement is very good even for the worst case. The small discrepancies can easily be explained. The small discontinuity near the 5-percent chord location is caused by the presence of the boundary layer transition strip. The pressure orifice at the 41-percent chord on the upper surface leaked during the NASA tests. It is possible similar problems occurred during the NAE tests.

The chordwise shock location is sensitive to wall interference. It is a useful gauge to assess the agreement of the results, especially when the test conditions differ slightly. Different methods have been used to define shock location. A sketch showing the method used is presented in figure 8a. A straight line was drawn through the pressure distribution in the area just ahead of the shock, through the shock, and just behind the shock. The intersection of the line upstream of the shock and the line through the shock defined the upstream limit of the shock region. Similarly, the intersection of the line downstream of the shock and the line through the shock defined the downstream limit of the shock region. The average shock location, x_s, corresponded to the mid-point of the shock region. The variation of the shock location with normal force coefficient is presented in figure 8b. The shock locations are in excellent agreement with each other, seldom differing by more than 2 percent chord.

The model chordwise pressure distributions and the momentum loss in the wake were integrated to obtain the section normal force, drag, and pitching moment coefficients. Two samples of these results are presented in figure 9. The drag coefficient was measured on the tunnel centerline. No corrections for the effect of flow angularity or for the interference from the sidewall boundary layer have been applied to these results. The pitching moment data are in very good agreement except near the stall. The drag coefficient at a given normal force coefficient is less for the NASA tests than for the NAE tests. Only a limited number of the NASA tests reached the stall. Of these results, the maximum normal force coefficient measured in the NASA tests is greater in all cases except one. Examination of the spanwise distribution of the drag coefficient shows the flow in the wake is not two-dimensional for many of the test conditions near the stall.

The slopes of the fairings of the section normal force curves have been calculated at $c_n = 0.2$, $c_n = 0.4$, and $c_n = 0.6$. The slope of the section normal force curve, c_{n_α}, should vary linearly with β^{-1}, the reciprocal of the Prandtl-Glauert compressibility factor, over the range of Mach numbers where linear aerodynamic theory is valid. The slopes have been plotted against β^{-1} rather than M_∞ for two reasons. At the smaller values of M_∞ (and β^{-1}), deviation from a linear relationship would indicate a problem in the results. At the larger values of M_∞ (and β^{-1}), the data would be spread out on the abscissa to permit closer inspection of the results for small Mach number changes. The calculated slopes are presented in figure 10. The level of agreement is reasonable. Except for the NAE results at $\beta^{-1} = 1.05$, (M_∞=0.30), the slopes vary linearly at the lower normal force coefficients and Mach numbers. The slope measured in the NASA tests is greater and the difference increases with Mach number. Both sets of results show the dramatic loss in slope at about the same Mach number.

The section drag coefficient has been cross-plotted against Mach number at constant values of section normal force coefficient. The results are plotted in figure 11. As noted previously, the drag at a given normal force is slightly less in the NASA tests. The difference in c_d is only 0.0004 over most of the Mach number range. The drag rise Mach number is difficult to determine because of non-uniformities in the curves. The drag rise appears to occur at a Mach number 0.01 lower in the NAE results.

Results Corrected for Sidewall Interference

The test section top and bottom walls and the sidewalls produce wall interference. The top and bottom wall interference has been accounted for in both the NAE and NASA results. Both sets of results contain residual interference, including that from the sidewalls. The model pressure distribution will lead to a local thinning and thickening of the sidewall boundary layer. The change in the sidewall boundary layer displacement thickness changes the blockage present in the empty test section calibration. Murthy has developed a correction method for this sidewall interference in conventional two-dimensional wind tunnels. This method, described in reference 11, is not directly applicable to an adaptive wall test section. In an adaptive wall test section, part of the blockage change from the sidewalls is felt in the pressures measured on the top and bottom walls. The wall adaptation scheme will compensate for that part of the blockage when it finds the proper wall shape. What portion of Murthy's correction needs to be applied has not yet been determined.

The results from both tests must be corrected for sidewall interference. The Murthy method, as implemented in the computer program of reference 12, was used to correct both sets of data for sidewall interference. Since the portion of the correction needed for the NASA results was unknown, the whole correction was applied as a limiting case. The slopes of the corrected normal force curves were computed at $c_n = 0.4$. The results are presented in figure 12. The corrected slopes are still in reasonable agreement. Both curves have been shifted slightly upward and to the left. The corrected drag coefficients have been crossplotted against the corrected Mach number at $c_n = 0.4$. The results are presented in figure 13. These results are also in reasonable agreement.

Comparison with Analytical Free Air Results

The results still differ slightly after corrections for the sidewall interference. A set of free air results is needed to determine the level of residual interference remaining in each set of data. Experiments to determine free air airfoil results at the desired Reynolds number and Mach number are not practical. For this study, analytical results will be used to approximate free air results. A coupled inviscid/viscid airfoil program, GRUMFOIL, was used to generate free air results. This program is described in reference 13. The results are presented in figure 13. The computed level of drag agrees more closely with the NASA results at the lower Mach numbers. The Grumfoil computed drag rise agrees more closely with the NAE results.

The adaptive wall alleviated the wall interference from the top and bottom walls. Correcting the data for sidewall interference improves the agreement with the analytical free air results. Some residual errors remain in one or both sets of data.

CONCLUDING REMARKS

A two-dimensional airfoil model has been tested in the adaptive wall test section of the NASA Langley 0.3-Meter Transonic Cryogenic Tunnel and in the National Aeronautical Establishment High Reynolds Number Two-Dimensional Facility. The primary goal of the tests was to assess two different wall interference alleviation and correction techniques: adaptive test section walls and classical analytical corrections. The wall interference in the NASA tests has been alleviated by the movement of the top and bottom walls. The wall interference in the NAE tests has been corrected by classical analytical techniques. The results can be summarized as follows:

1. The shock locations are in excellent agreement.

2. The NASA results had a lower drag coefficient at a given normal force coefficient. The drag rise for the NASA results occurs at a higher Mach number.

3. The slopes of the normal force curves were in reasonable agreement where linear aerodynamic theory is valid. At the higher Mach numbers, the NASA slopes were slightly greater.

4. Correcting the results for sidewall interference improves the agreement of the results with the analytical results.

5. The adaptive wall was successful in alleviating the top and bottom wall interference. Corrections for the effects of the sidewall interference are needed to approach free air results.

ACKNOWLEDGMENTS

I would like to express my appreciation to the staff of the NAE High Speed Aerodynamics Laboratory. Their assistance and cooperation in all aspects of the tests insured a successful test program. Special thanks are extended to Dr. Louis Chan of the NAE for the thorough tests at the NAE and his assistance during the tests at NASA. I would like to thank Mr. Edward Ray of the Experimental Techniques Branch at NASA for his technical review of this paper.

REFERENCES

1. Two-Dimensional Wind Tunnel Wall Interference, AGARD-AG-281, November 1983.

2. Brown D.: Information for Users of the National Research Council's 5 ft x 5 ft Blowdown Wind Tunnel at the National Aeronautical Establishment. NRC/NAE LTR-HA-6, Third edition, September 1977.

3. Ohman, L. H.: The NAE High Reynolds number 15 in. x 60 in. Two-Dimensional Test Facility. Part 1. General Information NRC/NAE Laboratory Technical Report LTR-HA-4, April 1970.

4. Chan, Y. Y.: Wind Tunnel Investigation of the CAST-10-2/DOA-2 12% Supercritical Airfoil Model. NAE Laboratory Technical Report LTR-HA-5x5/0162. May 1986.

5. Mokry, M.; and Ohman, L. H.: Application of Fast Fourier Transform to Two-Dimensional Wind Tunnel Wall Interference. Journal of Aircraft, Vol. 17, No. 6, June 1980, pp.402-408.

6. Ladson, Charles L.; and Ray, Edward J.: Evolution, Calibration, and Operational Characteristics of the Two-dimensional Test Section of the 0.3-Meter Transonic Cryogenic Tunnel. NASA TP 2947, September 1987.

7. Mineck, Raymond E.: Wall Interference Tests of a CAST 10-2/DOA 2 Airfoil in an Adaptive-Wall Test Section. NASA TM 4015, November, 1987.

8. Judd, M.; Wolf, S. W. D.; and Goodyer, M. J.: Analytical Work in Support of the Design and Operation of Two Dimensional Self-Streamlining Test Sections. NASA CR-145019. 1976.

9. Seraudie, A.; Blanchard, A.; Briel, J. F.: Rapport d'essais du Profil CAST 10 en Transition Declenchee Effectues dans la Soufflerie Transsonique Cryogenique T2 en Presence de Parois Auto-adaptables. ONERA R.T. OA 63/1685 AND. 1985.

10. Braslow, A. L.; and Knox, E. C.: Simplified Method for Determination of Critical Height of Distributed Roughness Particles for Boundary Layer Transition at Mach Numbers from 0 to 5. NASA TN 4363. 1958.

11. Murthy, A. V.: Effect of Aspect Ratio on Sidewall Boundary Layer Influence in Two-Dimensional Airfoil Testing. NASA CR 4008. September 1986.

12. Murthy, A. V.: A Simplified Fourwall Interference Assessment Procedure for Airfoil Data Obtained in the Lamgley 0.3-Meter Transonic Cryogenic Tunnel. NASA CR 4042. January 1987.

13. Melnik, R. E.; Chow, R. R.; Mead, H. R.; and Jameson, A.: An Improved Viscid/Inviscid Interaction Procedure for Transonic Flow Over Airfoils. NASA CR-3805. October 1985.

TABLE 1

Airfoil Model Ordinates

Upper Surface			Lower Surface		
x/c	z/c design	z/c measured	x/c	z/c design	z/c measured
.0000	.0034	.0034	.0001	.0034	.0034
.0003	.0062	.0063	.0004	.0004	.0004
.0015	.0094	.0093	.0014	-.0021	-.0021
.0033	.0124	.0123	.0031	-.0043	-.0043
.0063	.0159	.0158	.0061	-.0066	-.0065
.0140	.0217	.0217	.0096	-.0081	-.0081
.0195	.0250	.0251	.0153	-.0099	-.0099
.0247	.0279	.0279	.0273	-.0127	-.0128
.0356	.0331	.0332	.0339	-.0141	-.0142
.0470	.0376	.0377	.0470	-.0169	-.0169
.0654	.0432	.0433	.0673	-.0205	-.0206
.0846	.0478	.0478	.0874	-.0238	-.0238
.1179	.0536	.0536	.1148	-.0277	-.0277
.1519	.0580	.0580	.1562	-.0328	-.0329
.2139	.0633	.0633	.2741	-.0446	-.0447
.2764	.0665	.0665	.3366	-.0492	-.0492
.3321	.0681	.0681	.3919	-.0520	-.0520
.3949	.0689	.0689	.4539	-.0532	-.0532
.4576	.0686	.0685	.5161	-.0520	-.0520
.5132	.0673	.0672	.5714	-.0489	-.0488
.5757	.0645	.0644	.6340	-.0436	-.0436
.6376	.0601	.0600	.6967	-.0373	-.0374
.6925	.0542	.0541	.7525	-.0316	-.0317
.7539	.0453	.0452	.8149	-.0255	-.0257
.8152	.0338	.0337	.8775	-.0204	-.0206
.8763	.0203	.0202	.9189	-.0177	-.0178
.9172	.0106	.0105	.9468	-.0162	-.0164
.9511	.0024	.0024	.9743	-.0151	-.0152
.9782	-.0042	-.0042	1.0000	-.0145	-.0146
1.0000	-.0095	-.0095			

TABLE 2

Adaptive Wall Method Convergence Criteria

1	Average C_p error, top wall	Less than 0.01
2	Average C_p error, bottom wall	Less than 0.01
3	Induced angle of attack	Less than .015°
4	Induced camber	Less than .07
5	Average C_p error along model chord	Less than .007

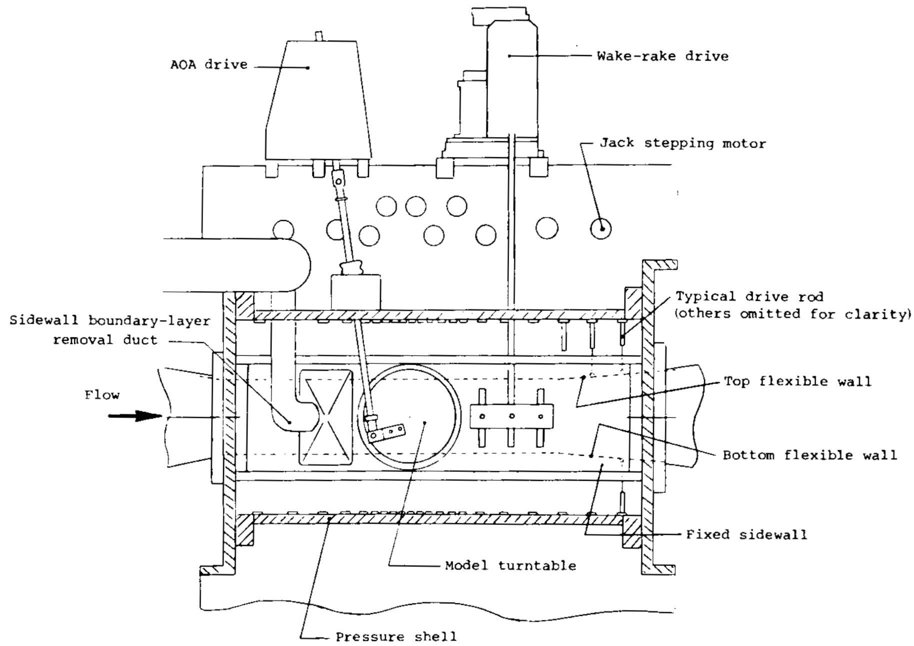

Figure 1. Details of the NASA Langley 13 inch by 13 inch adaptive wall test section. (Plenum sidewall removed).

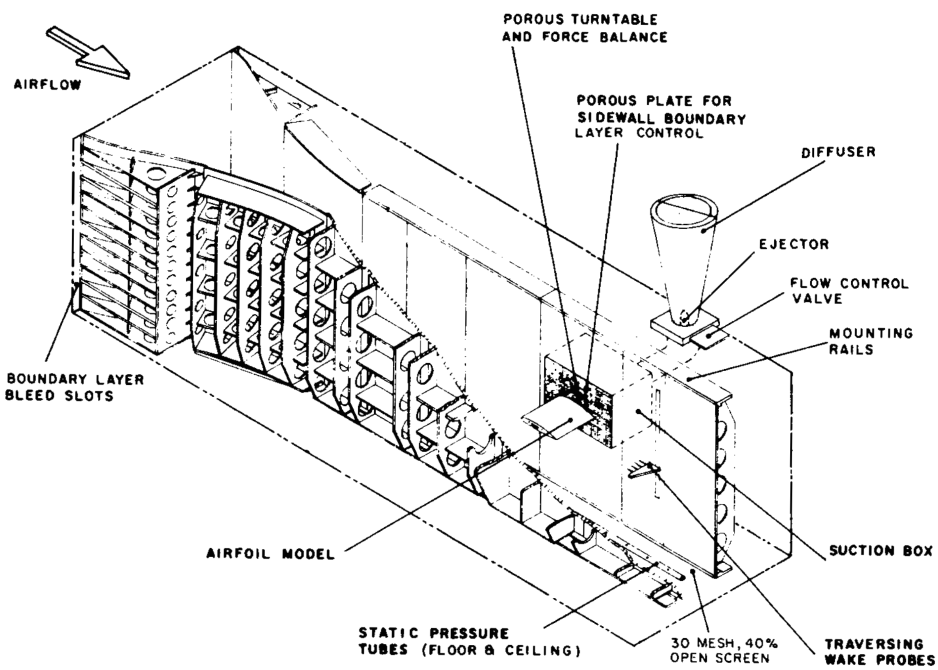

Figure 2. Details of the NAE 15 inch by 60 inch Two-dimensional High Reynolds Number Facility.

ORIGINAL PAGE IS
OF POOR QUALITY

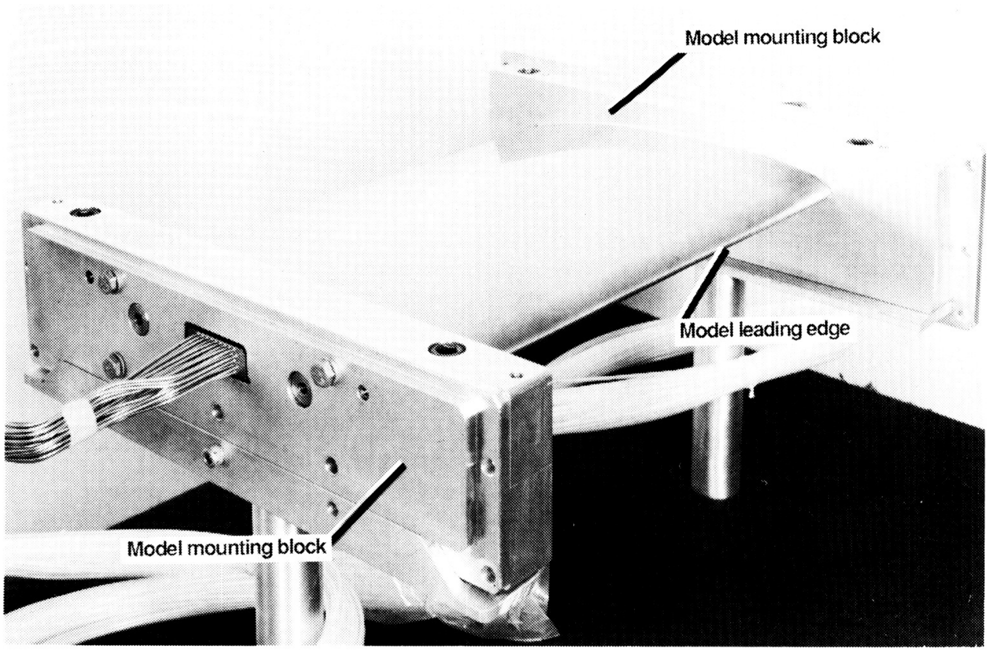

Figure 3. CAST 10-2/DOA 2 airfoil model with the model mounting blocks for the NASA tests.

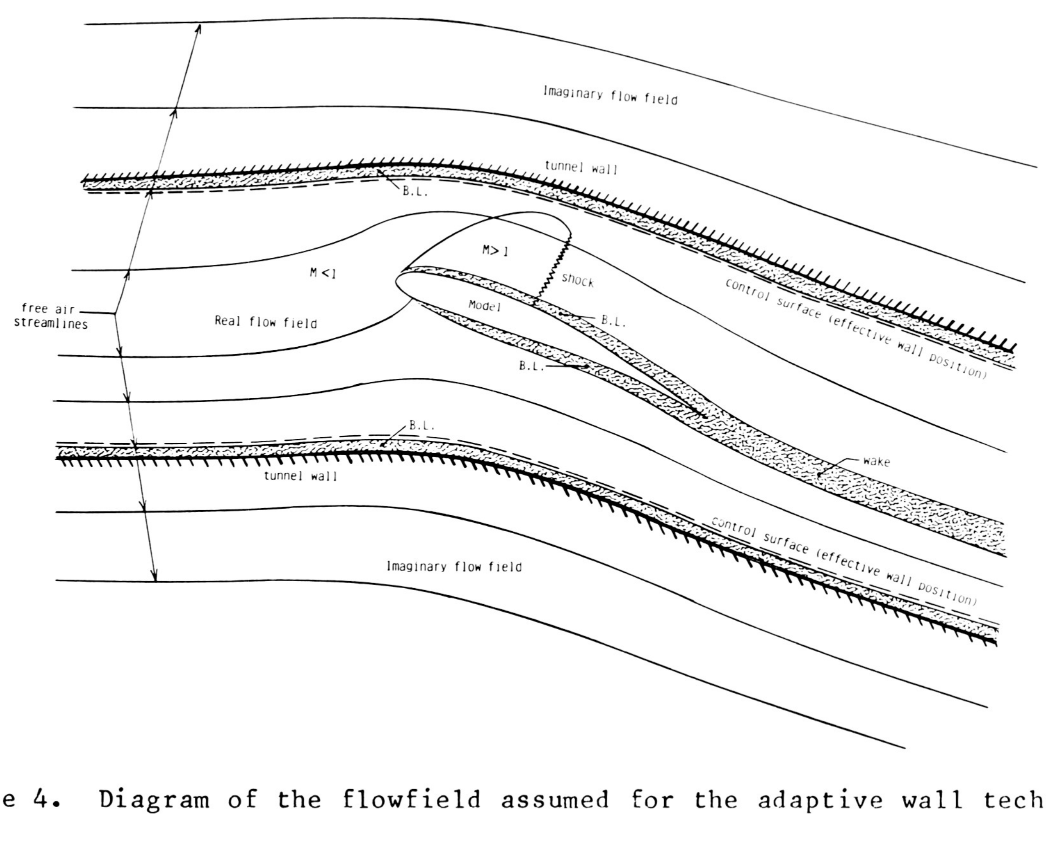

Figure 4. Diagram of the flowfield assumed for the adaptive wall technique.

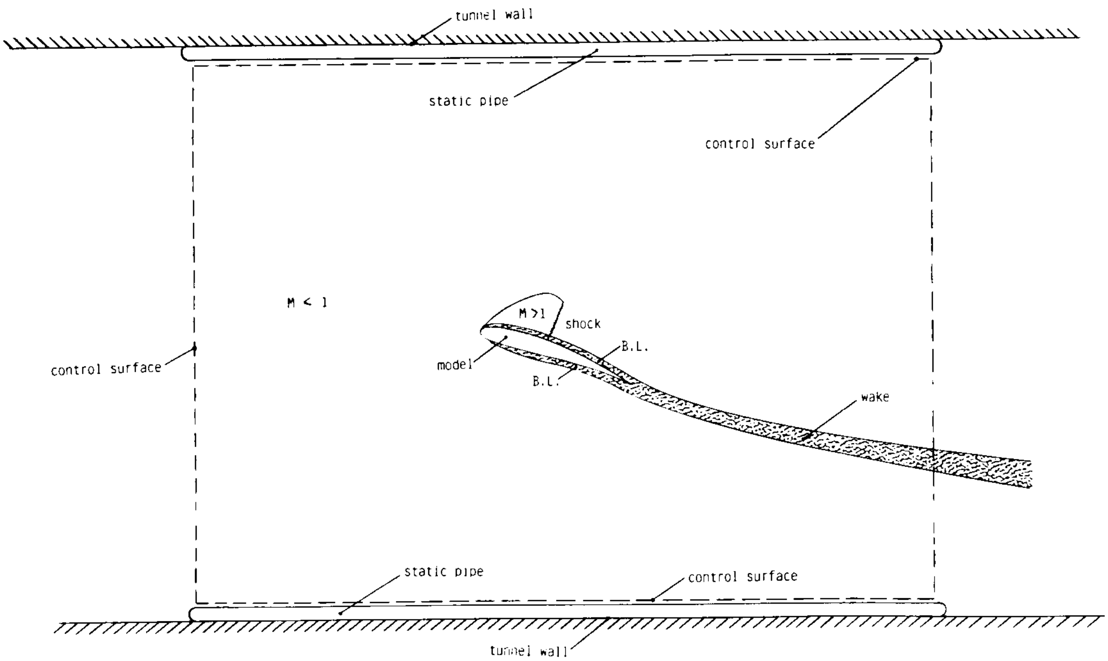

Figure 5. Diagram of the flowfield assumed for the NAE wall interference correction technique.

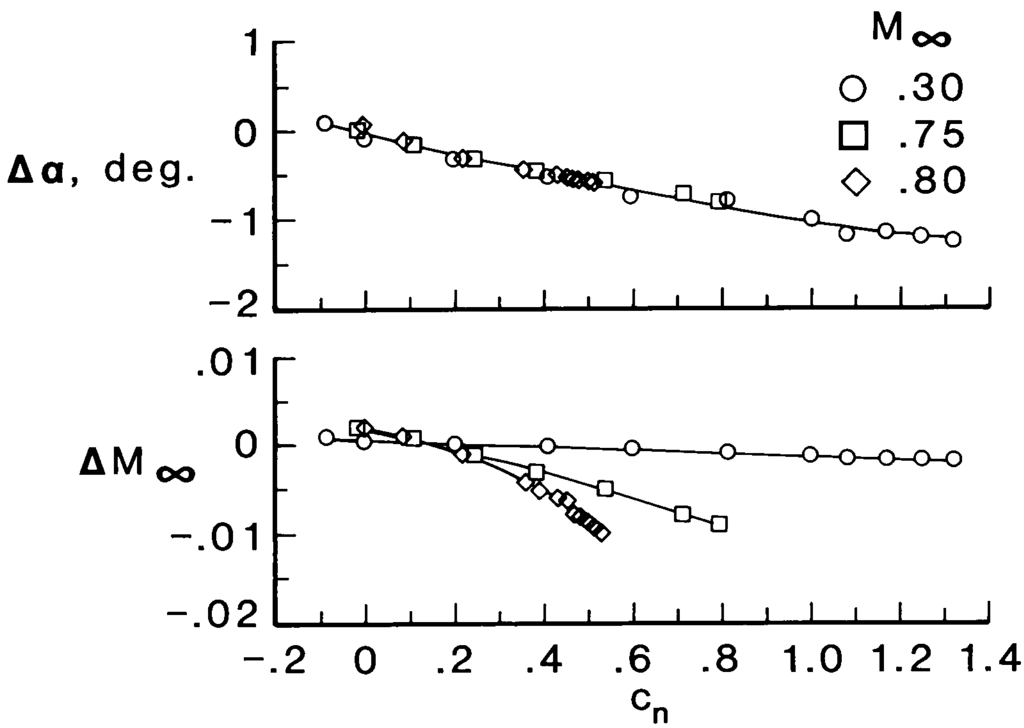

Figure 6. Corrections applied to NAE data for top and bottom wall interference. $R_c = 10 \times 10^6$.

ORIGINAL PAGE IS
OF POOR QUALITY

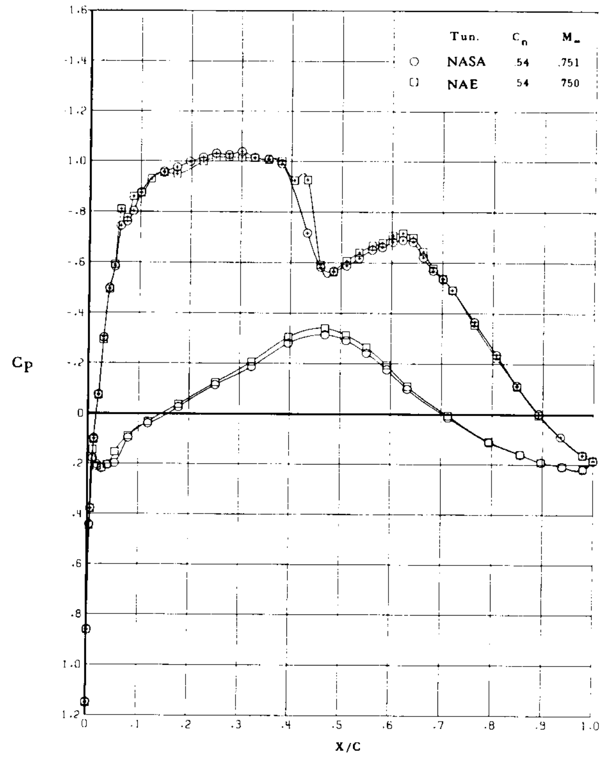

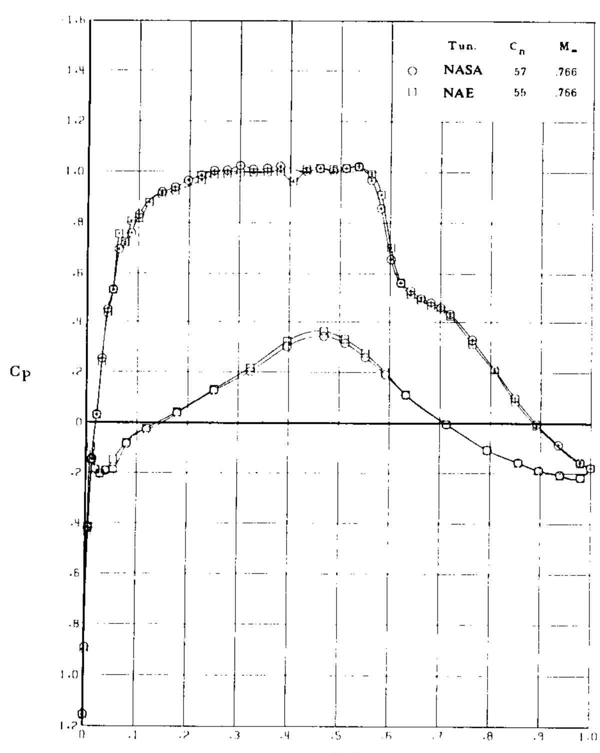

Figure 7. Comparison of the chordwise pressure distributions. $R_c = 10 \times 10^6$.

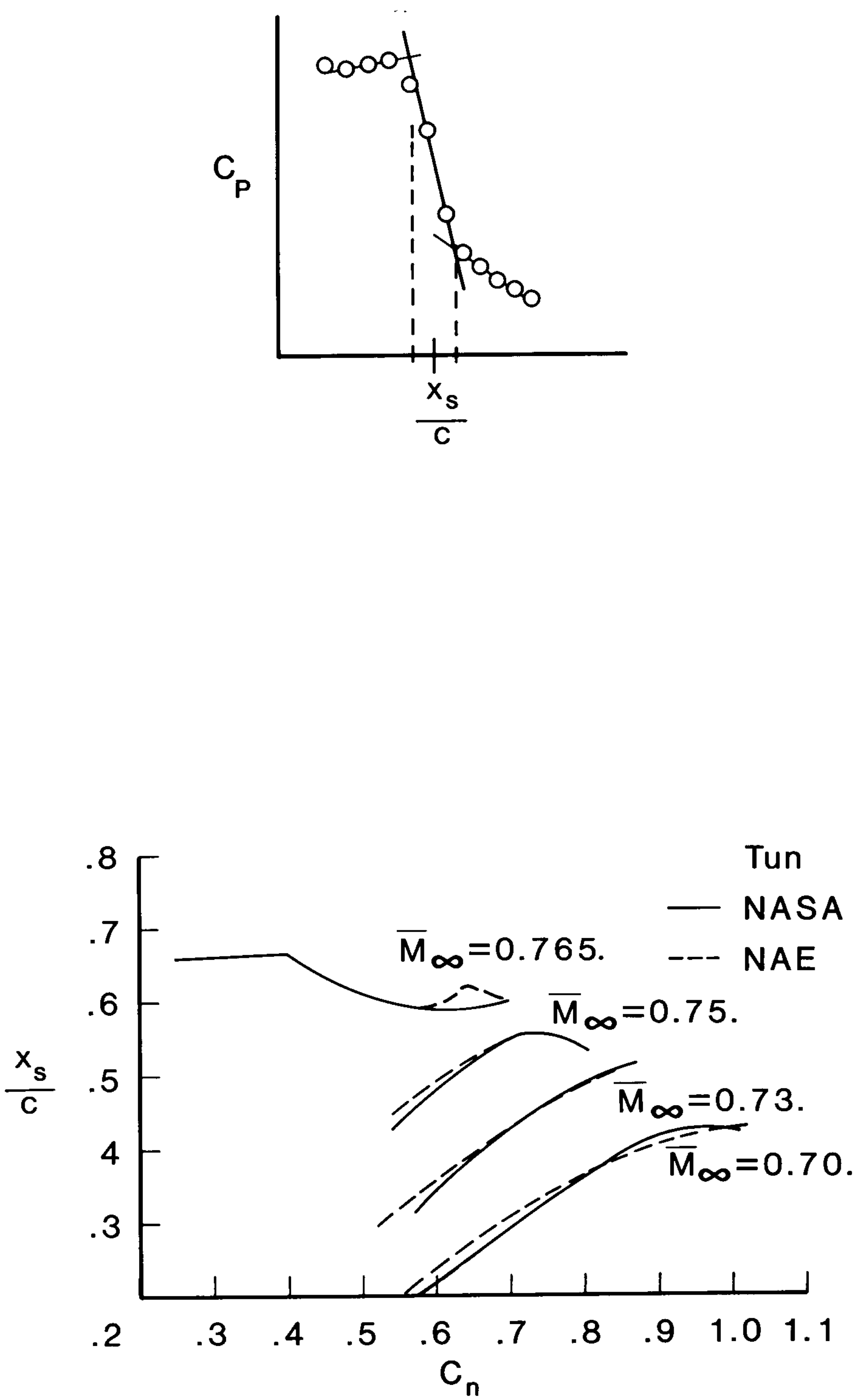

Figure 8. Comparison of the shock position. $R_c = 10 \times 10^6$.

ORIGINAL PAGE IS
OF POOR QUALITY

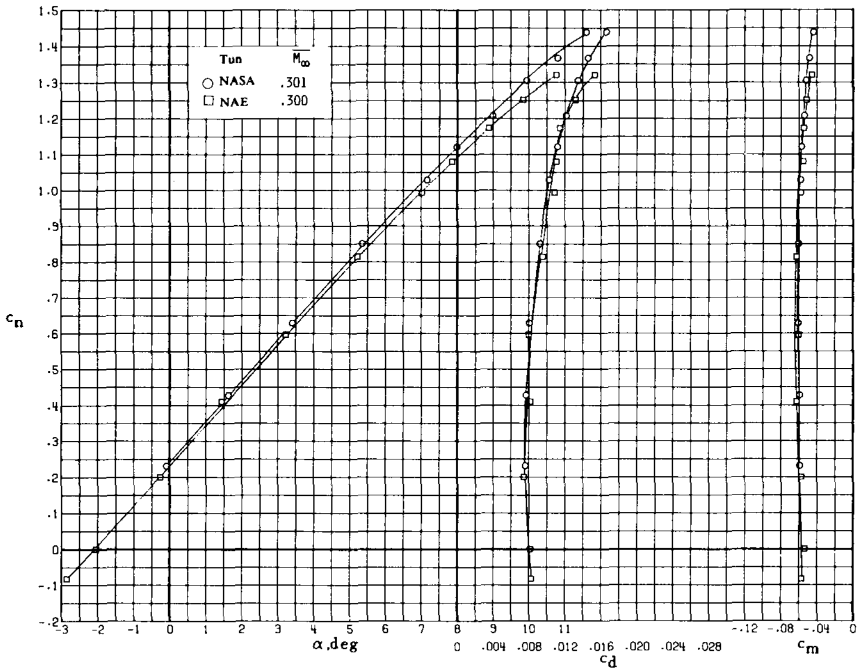

(a) M_∞ = 0.30.

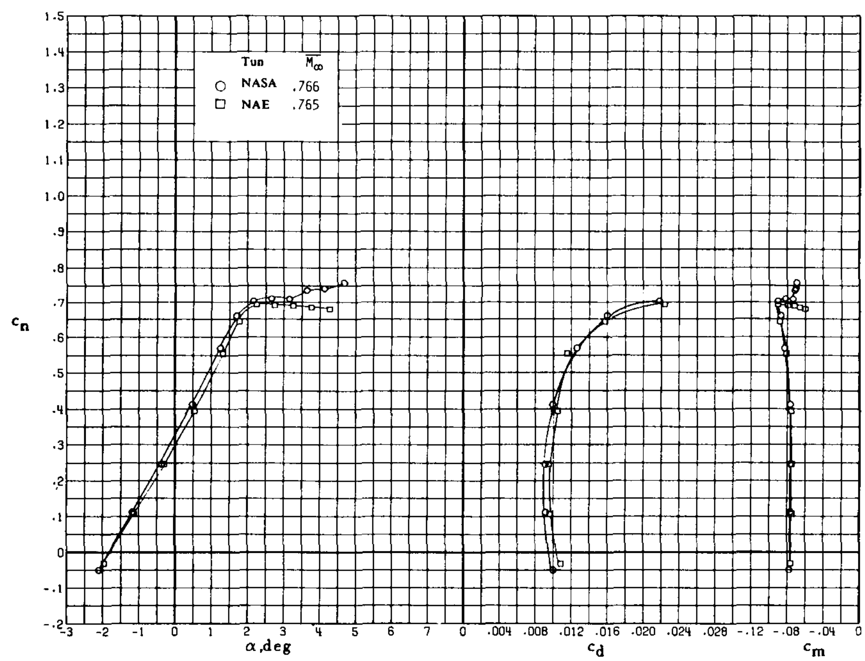

(b) M_∞ = 0.765.

Figure 9. Comparison of the integrated forces and moments. $R_c = 10 \times 10^6$.

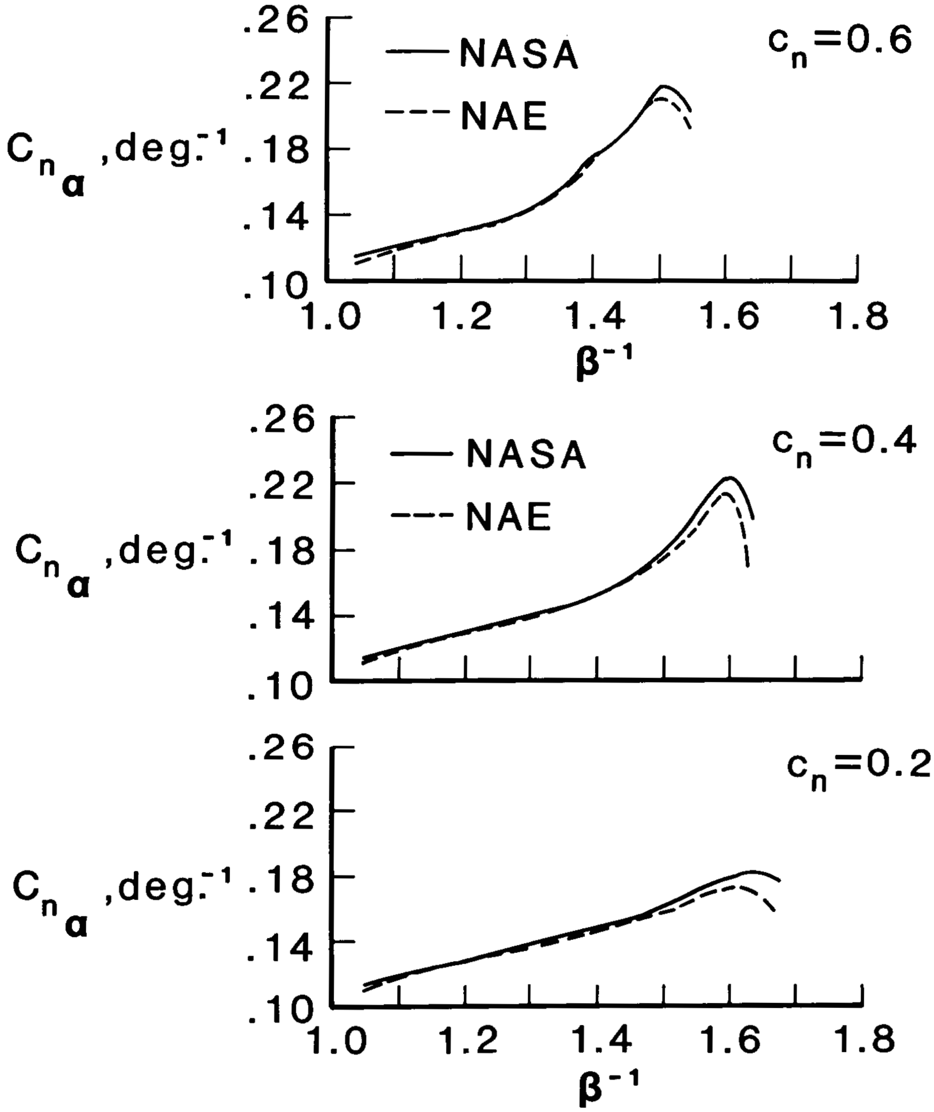

Figure 10. Comparison of the slopes of the normal force curves. $R_c = 10 \times 10^6$.

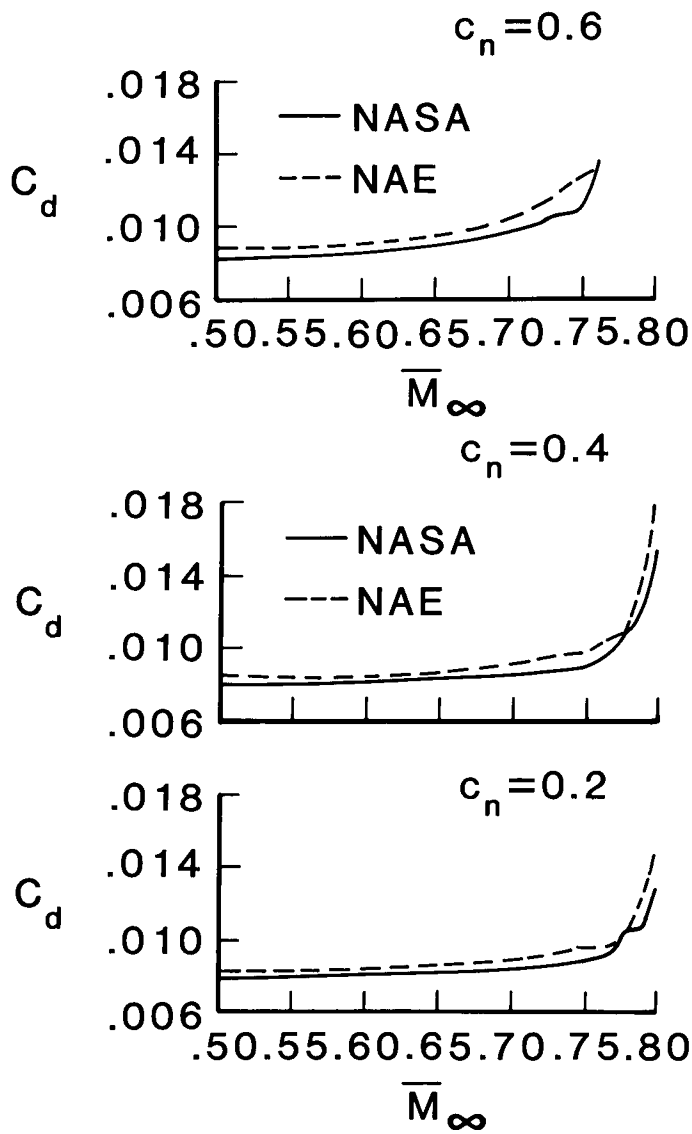

Figure 11. Comparison of the drag rise characteristics. $R_c = 10 \times 10^6$.

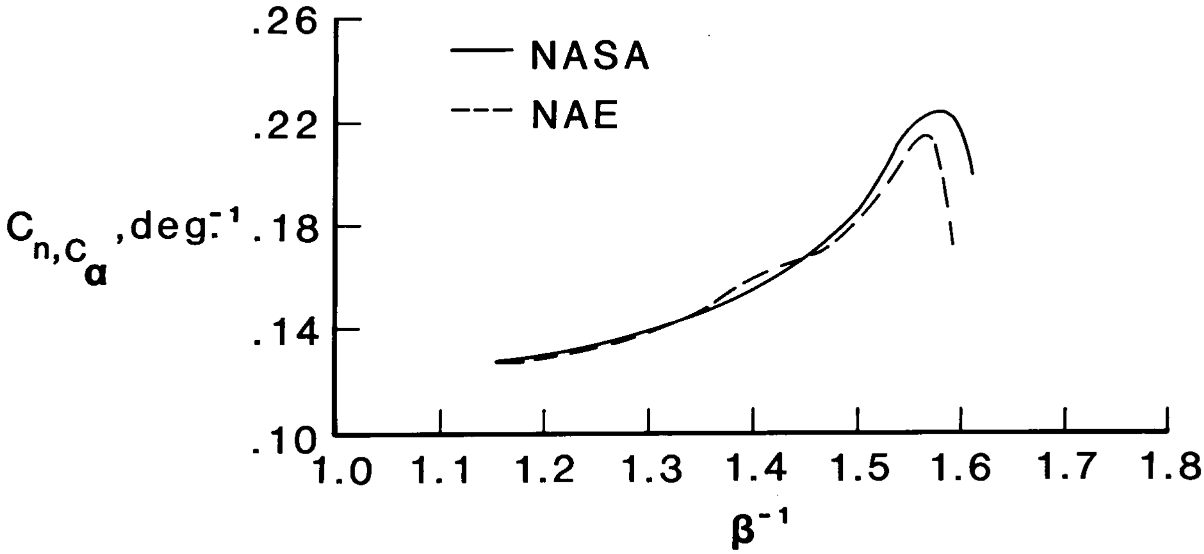

Figure 12. Comparison of slopes of the normal force curves corrected for sidewall interference with theory. $R_c = 10 \times 10^6$.

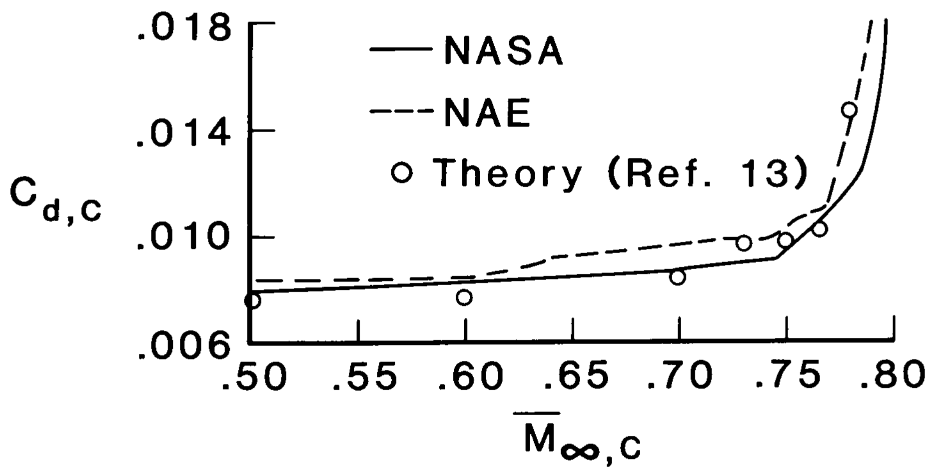

Figure 13. Comparison of the drag rise characteristics corrected for sidewall interference with theory. $R_c = 10 \times 10^6$.